

Shape and extinction thresholds in sonoluminescence parameter space

Jeffrey A. Ketterling* and Robert E. Apfel

Department of Mechanical Engineering, Yale University, New Haven, Connecticut 06520
ketterling@rrnyc.org, robert.apfel@yale.edu

Abstract: Experimental single bubble sonoluminescence (SBSL) ambient radius, acoustic drive pressure (R_o - P_a) phase diagrams are compared with predictions of the Dissociation Hypothesis (DH) and calculations of the $n = 2, 3, 4$ shape thresholds, focusing on the location of unstable SBSL and the extinction threshold. A phase diagram for experimental runs with a 20% air saturation is shown to indicate the location of the SBSL extinction threshold. Mixtures with appropriate concentrations of argon and nitrogen are presented to show the location of unstable SBSL. The results are consistent with the DH and show that unstable SBSL and the extinction threshold appear to coincide more closely with the $n = 4$ shape threshold.

©2000 Acoustical Society of America

PACS numbers: 43.35.Ei, 78.60.Mq

1. Introduction

A single, gas-filled bubble in the presence of an acoustic standing wave can emit a pulse of light as the bubble violently collapses each acoustic cycle. This process has been labeled single bubble sonoluminescence (SBSL).¹ Some of the interesting early observations concerning SBSL were the need for a noble gas to obtain light emission,² the apparent violation of mass diffusion for a single stable bubble,³ and a “dissolution island” in parameter space where stable bubbles were observed when they would normally be expected to dissolve.⁴ These observations helped to support what is commonly referred to as the Dissociation Hypothesis (DH) of SBSL.^{5–8}

DH permits predictions of bubble behavior in the ambient radius, acoustic drive pressure (R_o - P_a) parameter space under the assumption that the diatomic gases in the bubble begin to dissociate as P_a increases and the bubble collapse becomes more violent. Stable non-SL occurs at lower P_a , as the bubble enters a stable dissociation equilibrium where the amount of diatomic gas dissociated each acoustic cycle equals the amount diffusing back into the bubble. In parameter space, the calculated dissociation equilibrium has a negative slope. Stable SL occurs at higher P_a , once all of the diatomic gases have “burned” off, and the bubble enters a stable diffusive equilibrium based on the noble gas content remaining in the bubble. In parameter space, the calculated stable diffusive equilibrium has a positive slope.

The predictions of DH for stable bubble behavior agree very well with experimental results.^{9–11} For sufficiently high noble gas concentrations, DH also predicts that unstable SL will occur as the bubble intersects a shape stability threshold as it grows by rectified diffusion,¹² just as bubbles do under low P_a , non-SL conditions.^{4,9} In this letter, we show experimental results for air and argon-nitrogen mixtures and compare them with calculations of the shape stability threshold. A brief background of DH as it relates to shape instabilities is given, and the experimental apparatus is summarized. The experimental results are then presented.

*Present address: Riverside Research Institute, 330 West 42nd Street, New York, NY, 10036

2. Background

There exist regions of R_o - P_a parameter space where shape instabilities are likely.^{4,5,13-15} In DH, the shape stability threshold (SST) acts as the upper bound for unstable SL and non-SL bubbles. However, the first mode to set in ($n = 2$) may not be sufficient to cause the bubble to “dance” or break up. Therefore, we also consider higher order modes. When the bubble reaches a SST, several things may happen. First, it may become unstable and pinch off a microbubble causing it to drop to a lower R_o and then grow back in size until it intersects the SST again. This behavior is sometimes referred to as “dancing.”^{1,4,16} Second, the bubble may remain oscillating in a “stable” fashion for a long time period with the resonant mode present.^{4,17,18} This behavior becomes less likely with increasing mode number, because higher order modes have increased damping. Finally, a fast time scale instability may step in and cause the bubble to suddenly break up with a small change in P_a .¹⁹ The sudden break up of the bubble is often referred to as the SL extinction threshold. What initiates the sudden extinction is not well understood but may relate to the Rayleigh-Taylor instability,¹³ Richtmyer-Meshkov instability,²⁰ or the translation experienced by the bubble from the instantaneous Bjerknes force.^{19,21}

We will consider the SST to also act as the extinction threshold even though this may not be strictly true. The boundary in parameter space between where the SST causes unstable behavior and extinction is not clearly defined. Experimentally, extinction is more likely to occur at higher P_a .

A SST is defined as the location in parameter space where the amplitude of a shape mode of order n ($a_n(t)$) begins to maintain a steady, nonzero value.^{5,14,15} The location of the SSTs for $n = 2$ (solid with +), $n = 3$ (solid with \times), and $n = 4$ (solid with $*$) are shown in Fig. 1. These curves were calculated by Wu²⁰ at 33 kHz using the method described in Ref. 14. Recent calculations by Hao²² and Hilgenfeldt²³ agree with the $n = 2$ SST calculated by Wu.

3. Apparatus

The apparatus has been described in more detail elsewhere.^{10,11} It consisted of a cylindrical levitation cell acoustically excited at 32.8 kHz. Before running an experiment, fluid was prepared with a gas-handling system, which allowed accurate control of the gas content of the fluid. Once a bubble was levitated, its oscillation was captured with a stroboscopic imaging system (SIS).¹⁸ From the digital images acquired with the SIS, we were able to construct a time averaged radius-time $R(t)$ history of the bubble oscillation. From this curve we extracted a value for the maximum radius R_{max} ($\pm 1.1 \mu\text{m}$) and R_o ($\pm 0.9 \mu\text{m}$). These values were used to determine P_a ($\pm 0.07 \text{ atm}$) via a numerical fit to the Rayleigh-Plesset equation.¹⁰ Assembling the collection of $R(t)$ curves for a single gas saturation permitted the construction of a R_o - P_a phase diagram.

4. Results and discussion

4.1 Air saturated to 20%

Figure 1 shows a phase diagram for five experimental runs with a 20% air saturation. The final argon concentration in the fluid for this case is $C = 0.2\%$, where $C = 100\%$ would be complete saturation of the fluid. The data sets were taken over a period of several months which indicates the repeatability of the experiments. Each data point represents data from a single $R(t)$ curve. The data have one of four types of behavior: stable non-SL (square) (Mm. 1), unstable non-SL (circle) (Mm. 2), stable SL (upward pointing triangle) (Mm. 3), and unstable SL (downward pointing triangle) (Mm. 4).

Mm. 1. One cycle of typical stable non-SL captured with the SIS with $P_a \approx 1.25$ atm. Note the small R_{max} and the relatively strong afterbounces just after collapse. The horizontal width (true vertical) of the image is equivalent to $160 \mu\text{m}$. The duration of the acoustic cycle is $30.5 \mu\text{s}$, and the 75 frames of the animation are each separated by ≈ 400 ns. Light passing directly through the bubble causes the bright spot at the center the bubble (173 kb).

Mm. 2. One cycle of typical unstable non-SL captured with the SIS with $P_a \approx 1.1$ atm. Note that the bubble reaches a slightly larger R_{max} with the lower P_a , and the bubble tends to return to the same location. Afterbounces are also still visible (284 kb).

Mm. 3. One cycle of typical stable SL captured with the SIS with $P_a \approx 1.5$ atm. Note that R_{max} is now much larger, and afterbounces are weak because energy is lost to light emission (362 kb).

Mm. 4. One cycle of typical unstable SL captured with the SIS with $P_a \approx 1.6$ atm. Note the large R_{max} , the lack of strong afterbounces, and that the bubble tends to move along the same path. The unstable behavior is more "orderly" than that which was seen in Mm. 1 (324 kb).

Shown in the figure are the curves for the $C = 0.2\%$ diffusive equilibrium^{24,25} (solid), the stable dissociation equilibrium for 20% air (dash dotted) computed by Arlman,^{26,27} and the $n = 2, 3, 4$ SSTs (solid with +, \times , and $*$) calculated by Wu.²⁰ The behavior of the bubble with increasing P_a is described elsewhere¹⁰ and is similar to what has been reported by others.^{1,4,16} As DH predicts, the stable SL points agree with the $C = 0.2\%$ curve, and the stable non-SL points agree with the dissociation equilibrium.

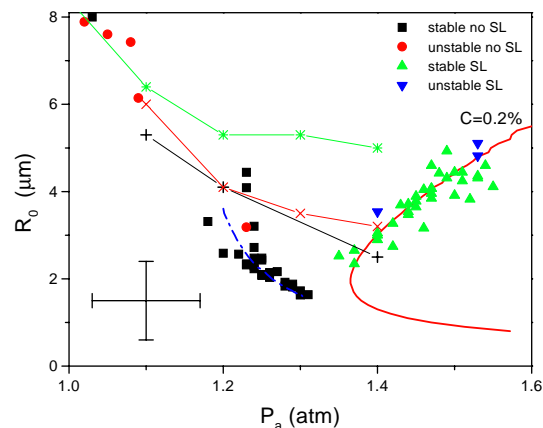


Fig. 1. Phase diagram for five experimental runs with air saturated to 20%. The curves represent theoretical calculations of the stable diffusive equilibrium $C = 0.2\%$ (solid), the stable dissociation equilibrium for a 20% air saturation computed by Arlman (dash dotted), and the $n = 2, 3, 4$ shape thresholds computed by Wu (solid with +, \times , and $*$). The bubble behavior is represented by a symbol shape (square, circle, upward pointing triangle, and downward pointing triangle). The cross hairs represent the experimental error.

In some of the runs, unstable SL was visible near the extinction threshold for SL. In these cases, the bubble was unstable, but the instability was not severe enough to destroy the bubble. Interestingly, SL bubbles appear stable well above the $n = 2, 3$ SSTs, and the extinction threshold appears to coincide with the $n = 4$ SST.

4.2 Argon-nitrogen mixture with $C = 1.2\%$ final argon concentration

To see unstable SL behavior over a wider pressure range, the argon concentration needs to be increased above $C \approx 0.7\%$.⁵ According to DH, as noble gas concentration increases, the diffusive stability curve takes on a more and more positive slope causing it to intersect the SST at lower and lower P_a . Because extinction does not usually occur at lower values of P_a (< 1.45 atm), the bubble instead follows the SST as P_a increases, undergoing repeated pinch off and growth until at some point it reaches the extinction threshold.

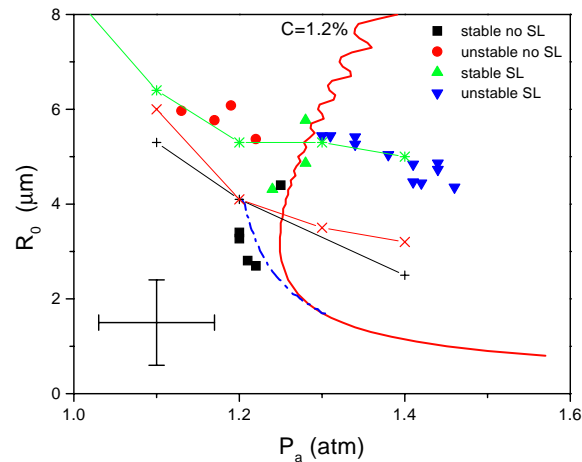


Fig. 2. Phase diagram for two experimental runs with a 12% argon and 88% nitrogen mixture saturated to 10%. The curves represent theoretical calculations of the stable diffusive equilibrium $C = 1.2\%$ (solid), the stable dissociation equilibrium for 10% air (dash dotted), and the $n = 2, 3, 4$ shape thresholds (solid with +, \times , and *).

Figure 2 shows the phase diagram for two 12% argon and 88% nitrogen mixtures saturated to 10%, which gives a final argon concentration in the fluid of $C = 1.2\%$. Also shown are the $n = 2, 3, 4$ SSTs (solid with +, \times , and *). As DH predicts, the stable SL points (upward pointing triangles) show agreement with the $C = 1.2\%$ curve (solid) until they intersect the $n = 4$ SST at $P_a \approx 1.3$ atm. Between $P_a = 1.3 - 1.45$ atm there is a region of unstable SL (downward pointing triangles) as also predicted by DH. For $P_a > 1.45$ atm, the bubble reaches the extinction threshold and rapidly breaks up.

For lower P_a where no SL is observed, it has been shown that the calculated $n = 2$ mode^{14,15} is in fairly good agreement with experimental data.⁴ The agreement is also seen for the $n = 3, 4$ modes, since all the modes lie fairly close together at low P_a . However, as seen in Fig. 2, the agreement between the data and the $n = 2$ mode does not appear to occur at higher P_a where SL was observed. This may imply that the higher order modes are more destructive to the bubble and contribute to unstable SL and SL extinction. It may also simply mean that the criterion used to define the SST^{5,14,15} is not sufficient to describe unstable behavior and extinction.

4.3 Argon-nitrogen mixture with $C > 2\%$ final argon concentration

With an amount of final argon concentration $C > 2\%$, DH predicts that neither stable SL nor stable non-SL should be observed. Figure 3 shows a phase diagram for two mixtures of $> 10\%$ argon in nitrogen saturated to 20%. The exact ratio of gases in the mixture was unknown due to an error in preparation. If we assume the initial gas mixture was 15% argon and 85% nitrogen, then the final argon concentration in the fluid would be

$C = 3\%$ (solid curve). This curve has no stable SL equilibria, and because it also nearly overlaps the dissociation equilibrium for 20% air (dash dotted), there is also no stable non-SL. Therefore, only unstable behavior is possible as was observed experimentally. Below $P_a \approx 1.3$ atm there were only “dancing”, nonluminescing bubbles (circles), and above $P_a \approx 1.3$ atm there were only unstable, luminescing bubbles. As in the previous case, the unstable SL behavior shows close agreement to the $n = 4$ SST (solid with *).

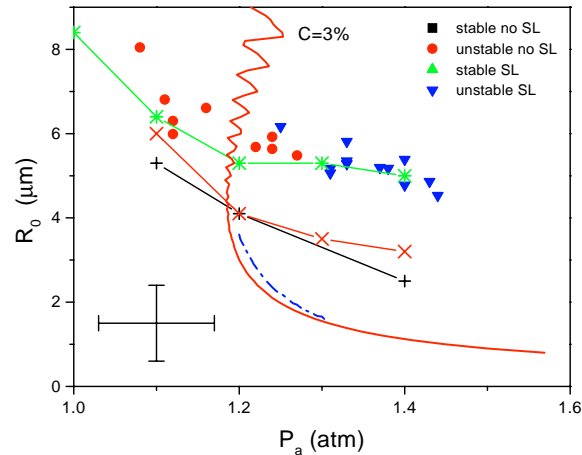


Fig. 3. Phase diagram for two experimental runs with an argon-nitrogen mixture having $> 10\%$ argon saturated to 20%. The curves represent theoretical calculations of the unstable diffusive equilibrium $C = 3\%$ (solid), the stable dissociation equilibrium for 20% air (dash dotted), and the $n = 2, 3, 4$ shape thresholds (solid with +, x, and *).

5. Conclusions

The experimental results presented here confirm that the predictions of DH for unstable SL are valid. For sufficiently high noble gas concentrations, the SST limits the growth of bubbles, resulting in “dancing” behavior. The SST also appears to coincide with the extinction threshold. The results raise new questions about what actually causes unstable bubble behavior and SL extinction. Previously, the $n = 2$ (quadrupole) mode was believed to be the cause;⁵ however, the work presented here suggests higher order modes may actually be more destructive to the bubble. In fact, we occasionally observed a luminescing bubble that appeared to have a shape instability, yet it showed no signs of “dancing”. Holt and Gaitan⁴ and Tian *et al.*¹⁸ have observed similar behavior, but for non-SL bubbles at lower P_a . These observations suggest that surfactants that suppress higher order shape modes²⁸ could be very useful for extending the region of stable SL in parameter space. Performing SBSL experiments in microgravity^{29–31} may also help stabilize the bubble by eliminating the translation induced by the Bjerknes force.²¹

Acknowledgements

We wish to acknowledge many valuable discussions with G. Holt, T. Matula, S. Hilgenfeldt, and R. Roy. We also wish to thank C. Wu, T. Arlman, and Y. Hao for sharing the results of their numerical calculations.

References and links

- ¹D. F. Gaitan, L. A. Crum, C. C. Church, and R. A. Roy, “Sonoluminescence and bubble dynamics for a single, stable, cavitation bubble,” *J. Acoust. Soc. Am.* **91**, 3166–3183 (1992).

- ²R. Hiller, K. Weninger, S. J. Putterman, and B. P. Barber, "Effect of noble-gas doping in single-bubble sonoluminescence," *Science* **266**, 248–250 (1994).
- ³R. Löfstedt, K. Weninger, S. Putterman, and B. P. Barber, "Sonoluminescing bubbles and mass diffusion," *Phys. Rev. E* **51**, 4400–4410 (1995).
- ⁴R. G. Holt and D. F. Gaitan, "Observation of stability boundaries in the parameter space of single bubble sonoluminescence," *Phys. Rev. Lett.* **77**, 3791–3794 (1996).
- ⁵S. Hilgenfeldt, D. Lohse, and M. P. Brenner, "Phase diagrams for sonoluminescing bubbles," *Phys. Fluids* **8**, 2808–2826 (1996).
- ⁶D. Lohse, M. P. Brenner, T. F. Dupont, S. Hilgenfeldt, and B. Johnston, "Sonoluminescing air bubbles rectify argon," *Phys. Rev. Lett.* **78**, 1359–1362 (1997).
- ⁷D. Lohse and S. Hilgenfeldt, "Inert gas accumulation in sonoluminescing bubbles," *J. Chem. Phys.* **107**, 6986–6997 (1997).
- ⁸S. Hilgenfeldt, S. Grossmann, and D. Lohse, "A simple explanation of light emission in sonoluminescence," *Nature* **398**, 402–404 (1999).
- ⁹D. F. Gaitan and R. G. Holt, "Experimental observations of bubble response and light intensity near the threshold for single bubble sonoluminescence in an air-water system," *Phys. Rev. E* **59**, 5495–5502 (1999).
- ¹⁰J. A. Ketterling and R. E. Apfel, "Experimental validation of the dissociation hypothesis for single bubble sonoluminescence," *Phys. Rev. Lett.* **81**, 4991–4994 (1998).
- ¹¹J. A. Ketterling, "An experimental validation of the dissociation hypothesis for sonoluminescence and an extension to the analysis of multiple frequency drives," Ph.D. dissertation, Yale University (1999).
- ¹²L. A. Crum, "Acoustic cavitation series part five - Rectified diffusion," *Ultrasonics* **22**, 215–223 (1984).
- ¹³M. P. Brenner, D. Lohse, and T. F. Dupont, "Bubble shape oscillations and the onset of sonoluminescence," *Phys. Rev. Lett.* **75**, 954–957 (1995).
- ¹⁴C. C. Wu and P. H. Roberts, "Bubble shape instability and sonoluminescence," *Phys. Lett. A* **250**, 131–136 (1998).
- ¹⁵A. Prosperetti and Y. Hao, "Modelling of spherical gas bubble oscillations and sonoluminescence," *Phil. Trans. R. Soc. Lond. A* **357**, 203–224 (1999).
- ¹⁶B. P. Barber, C. C. Wu, R. Löfstedt, P. H. Roberts, and S. J. Putterman, "Sensitivity of sonoluminescence to experimental parameters," *Phys. Rev. Lett.* **72**, 1380–1383 (1994).
- ¹⁷R. G. Holt, J. Holzfuss, A. Judt, A. Phillip, and S. Horsburgh, "Forced nonlinear oscillations of single air bubbles in water: Experimental results," In *Proc. of the 12th Int. Symp. on Nonlinear Acoustics, Austin, Texas*, M. Hamilton and D. Blackstock, eds., p. 497 (Elsevier, New York, 1990).
- ¹⁸Y. Tian, J. A. Ketterling, and R. E. Apfel, "Direct observation of microbubble oscillations," *J. Acoust. Soc. Am.* **100**, 3976–3978 (1996).
- ¹⁹S. M. Cordry, "Bjerknes forces and temperature effects in single-bubble sonoluminescence," Ph.D. dissertation, University of Mississippi (1995).
- ²⁰C. C. Wu, (private communication).
- ²¹T. J. Matula, S. M. Cordry, R. A. Roy, and L. A. Crum, "Bjerknes force and bubble levitation under single-bubble sonoluminescence conditions," *J. Acoust. Soc. Am.* **102**, 1522–1527 (1997).
- ²²Y. Hao, (unpublished data).
- ²³S. Hilgenfeldt, (unpublished data).
- ²⁴A. Eller and H. G. Flynn, "Rectified diffusion during nonlinear pulsations of cavitation bubbles," *J. Acoust. Soc. Am.* **37**, 493–503 (1965).
- ²⁵M. M. Fyrillas and A. J. Szeri, "Dissolution or growth of soluble spherical oscillating bubbles," *J. Fluid Mech.* **277**, 381–407 (1994).
- ²⁶T. Arlman, S. Hilgenfeldt, and D. Lohse, (preprint).
- ²⁷The curve is actually calculated for a mixture of 1% Xe and 99% nitrogen. However, since the nitrogen mainly influences the location of the curve, the curve for air would show little difference. The calculation includes the effect of water vapor on the internal temperature of the bubble.
- ²⁸T. R. Stottlemeyer and R. E. Apfel, "The effects of surfactant additives on the acoustic and light emissions from a single stable sonoluminescing bubble," *J. Acoust. Soc. Am.* **102**, 1418–1423 (1997).
- ²⁹R. G. Holt and R. A. Roy, "Sonoluminescence: The critical role of buoyancy in the stability and emission mechanisms," In *Proc. of the 4th Microgravity Fluid Phys. Conf.*, pp. 347–352 (NASA, 1998).
- ³⁰D. B. Thiessen, J. E. Young, M. J. Marr-Lyon, S. L. Richardson, C. D. Breckon, S. G. Douthit, P. S. Jian, W. E. Torruellas, and P. L. Marston, "Single bubble sonoluminescence in low gravity and optical radiation pressure positioning of the bubble," In *Proc. of the 4th Microgravity Fluid Phys. Conf.*, pp. 379–383 (NASA, 1998).
- ³¹T. J. Matula, (private communication).